Journal of Information Systems Engineering and Management
2025, 10(4)
e-ISSN: 2468-4376
https://www.jisem-journal.com/

Research Article

Hybrid Methodology for Blood Vessel Segmentation on Fundus Image: Frangi Filter, Otsu Thresholding and Morphological Operations

Hasnia Merzoug[1*], Hayat Yedjour[2]
[1]*Department of Management, University of Oran2, (Algeria).*
[2]*Department of Informatics, University of Sciences and Technology of USTO, Oran, (Algeria).*
[1,2]*ADASCA Laboratory, Computer Science Department, University of Science and Technology of Oran, Mohamed Boudiaf USTO.*
Corresponding author: merzoug.hasnia@univ-oran2.dz

ARTICLE INFO

Received: 27 March 2025

Revised: 13 May 2025

Accepted: 15 June 2025

ABSTRACT

Retinal vascular disease remains a significant medical concern, yet accurately segmenting blood vessels in fundus images continues to be challenging due to uneven lighting, low contrast, and the wide variability in vessel morphology—including very fine capillaries as well as broad arteries and veins .Automated segmentation not only improves diagnostic precision but also significantly reduces the manual workload of ophthalmologists, enhancing efficiency in both clinical and large-scale screening settings. This study aims to segment retinal blood vessels through a three-stage framework: Preprocessing: Improve image quality by applying CLAHE (Contrast Limited Adaptive Histogram Equalization) and a median filter to the green channel. Segmentation: Combine multiple techniques—Frangi filtering, 2D convolution, additional median filtering, Otsu's thresholding, morphological operations, and background subtraction—to robustly delineate vessel structures. The proposed model is evaluated using statistical parameters on images from two publicly available databases. We achieve average accuracies of 0.9418 and 0.9086 for DRIVE and STARE databases, respectively. These metrics indicate that the proposed model is an effective and viable alternative for retinal vessel segmentation, offering a strong balance of precision and practicality for clinical and research applications.

Keywords: Segmentation, Morphology, Frangi filter, Retinal, Blood vessels.

INTRODUCTION

Accurate segmentation of retinal blood vessels in fundus images is crucial for diagnosing various eye diseases, including diabetic retinopathy, glaucoma, and age-related macular degeneration [1]. Precise delineation of both primary vessels and their branches enables detailed analysis of vascular morphology, facilitating early detection and effective monitoring of these conditions.

Traditionally, ophthalmologists manually annotate blood vessels based on their expertise. This manual process is not only time-consuming but also susceptible to variability due to subjective judgment, potentially leading to inconsistencies in diagnosis. To address these challenges, automated retinal vessel segmentation methods have been developed. These techniques aim to enhance diagnostic accuracy and efficiency by providing consistent and objective analyses of retinal images [2]. By reducing reliance on manual annotation, automated systems can assist clinicians in making more reliable diagnoses and monitoring disease progression more effectively. Retinal fundus images often exhibit uneven grayscale distribution due to factors such as noise, artifacts, and varying illumination. This results in low contrast between blood vessels and the background, complicating accurate segmentation. Additionally, the overlapping and crossing of arteries and veins further hinder the segmentation process [3].

To address these challenges, two primary categories of blood vessel segmentation methods have been developed: supervised and unsupervised learning approaches. Supervised methods involve training models on labeled datasets, where the blood vessels have been manually annotated. These models learn to identify vessel patterns and can generalize to new, unseen images. Common supervised approaches include Convolutional Neural Networks (CNNs), Fully Convolutional Networks (FCNs), and U-Net architectures. While these methods often achieve high accuracy, they require substantial labeled data and computational resources [4]. Unsupervised methods do not rely on labeled data.

Journal of Information Systems Engineering and Management
2025, 10(4)
e-ISSN: 2468-4376
https://www.jisem-journal.com/

Research Article

Instead, they utilize image processing techniques and predefined rules to segment blood vessels. These approaches often involve filtering, thresholding, and morphological operations to enhance and extract vessel structures. While unsupervised methods are less dependent on annotated datasets, they may struggle with accurately detecting fine vessels and can be sensitive to image quality variations [5]. in summary, both supervised and unsupervised methods have their advantages and limitations. The choice between them depends on factors such as the availability of labeled data, computational resources, and the specific requirements of the segmentation task.

Despite notable advances in segmentation techniques, practical implementation remains difficult due to several persistent issues. Image quality can suffer from noise during acquisition, compression artifacts, low contrast, uneven illumination, and wide variations in vessel diameter—factors that often lead to broken vessel structures and misclassified pixels. Additionally, individual retinal morphology—including both healthy and pathological variations—introduces further unpredictability. Features such as lesions, the optic disc, vessel bifurcations, and crossovers pose challenges even for supervised models. Moreover, constructing a comprehensive training set that captures the full spectrum of these imaging and anatomical variations is incredibly difficult. This limitation constrains the capacity of classifiers and hampers the overall performance of automated systems [6]. Consequently, the primary challenge remains: developing a segmentation approach that is both simple to implement and reliably accurate across diverse image qualities and retinal variations.

In this work, we present a novel hybrid model for the automatic and precise segmentation of retinal vasculature, which harnesses the strengths of unsupervised approaches. Our focus lies in enhancing both pre-processing and post-processing stages: traditional techniques are employed to normalize illumination and contrast, while post-processing is used to remove disconnected or irrelevant components from the detected vessel network. This structured pipeline combines robustness to noise and variability with computational efficiency [7].

First, we extract the green channel from each fundus image, as this channel offers higher contrast between the blood vessels and the background, making their detection easier. On this channel, we then apply the CLAHE method (Contrast Limited Adaptive Histogram Equalization) to normalize the lighting and effectively enhance edges, particularly in regions with strong anisotropy or low local contrast. Finally, a median filter is used to reduce noise while preserving the fine vascular structures before the subsequent segmentation steps. Following preprocessing, a hybrid segmentation approach is applied to each image. This consists of: (1) enhancement with a Frangi vesselness filter, (2) feature extraction via a 2D convolutional filter, and (3) further filtering using a finite impulse response (FIR) filter—also referred to as an UOI filter. The enhanced image is then binarized using Otsu's thresholding, followed by morphological post-processing to refine vessel connectivity and eliminate spurious regions.

In the following section, we review previous studies on retinal blood vessels segmentation. Section 3 presents materials and details of the methodology used in this article. Section 4 discusses the experimental results obtained with our model and compares them to recent methods. Finally, we conclude this work in section 5.

1. Related work

Retinal images are frequently affected by various types of noise, such as Poisson or Gaussian noise, which stem from sensor imperfections or digitization artifacts. To enhance image quality, it is essential to apply preprocessing techniques, including illumination correction and artifact removal. Common approaches include mean, median, and Gaussian filtering, as well as contrast enhancement methods like histogram equalization [8]. Numerous studies have demonstrated that effective preprocessing significantly improves the accuracy of retinal blood vessel segmentation. These preprocessing steps often involve contrast enhancement through transformations applied in the spatial, frequency, or temporal domains. One particularly effective approach is contrast adjustment using wavelet transforms, which leverage time-frequency multiresolution analysis [9]. Asem et al. [10] employed such multiresolution techniques for image denoising. Compared to conventional spatial enhancement methods, wavelet-based techniques have been shown—by Zhen et al. [11], Bankhead et al. [12], and Zhang et al. [9] to substantially improve edge detection and overall image quality.

Despite their effectiveness, conventional transforms have shown limitations in accurately representing objects with pronounced anisotropic characteristics. To address these shortcomings, the Curvelet Transform was developed as a more suitable alternative to separable wavelet transforms for capturing curved structures and edges. This transform has proven highly effective in a range of image processing applications, particularly in enhancing visual quality.

Journal of Information Systems Engineering and Management
2025, 10(4)
e-ISSN: 2468-4376
https://www.jisem-journal.com/

Research Article

Distinguished by its localization in the spatial, frequency, and directional domains, the Curvelet Transform demonstrates strong sensitivity to directional and anisotropic features [13].A notable implementation of this method, the Fast Discrete Curvelet Transform (FDCT), excels at efficiently capturing object boundaries, lines, curves, and edges across multiple orientations. It was utilized by Rahulkar et al. [14] for feature extraction and by Altan et al. [15] as a core technique for image contrast enhancement when combined with other processing models. In pursuit of further improvements in segmentation accuracy, various researchers such as Soares et al. [16], Aslan et al. [17] and Fang et al. [18] have adopted image transformation techniques based on advanced filters and Gabor wavelets. Gabor filters, mathematically defined as the product of a sinusoidal (or harmonic) wave and a Gaussian envelope, function as effective detectors of edges, lines, and shapes. Their key advantage lies in their ability to adapt to varying spatial frequencies and orientations, making them particularly well-suited for feature detection tasks in complex images [19].

In general, vascular system segmentation techniques can be classified into two main categories: supervised and unsupervised methods [20]. Unsupervised methods operate without the need for labeled training data. Instead, they rely on a range of morphological operations to analyze and segment retinal images. For instance, Tavakoli et al. [21] proposed an unsupervised automated method for extracting retinal vasculature by employing morphological operators during the preprocessing stage to enhance the vessel structure. The main processing stage involved the application of the Radon transform on overlapping image windows, followed by refinement and reconstruction steps to produce the final binarized vessel map. Similarly, Dash and Bhoi [22] introduced a recursive strategy for segmenting ophthalmoscopic images. Their method began with gamma correction, followed by contrast enhancement using CLAHE. They then applied an iterative adaptive thresholding algorithm to extract the vascular structures. The final segmentation results, characterized by high average precision, were further refined using morphological cleaning operations.

Ravichandran et al. [23] proposed a fully automated method for blood vessel extraction based on enhancement and thresholding techniques. The input images were first enhanced using histogram matching and CLAHE (Contrast Limited Adaptive Histogram Equalization). To suppress background noise, Wiener filtering was applied. Subsequently, Gabor filter responses derived from the CLAHE-enhanced images were processed using a local entropy-based thresholding technique to extract the retinal vasculature. Similarly, Saleh et al. [24] focused on key preprocessing steps, including contrast enhancement and thresholding, to develop an automatic retinal vessel segmentation pipeline. Dash et al. [20] utilized Mean-C thresholding to extract the vascular network after improving the performance of the Curvelet Transform through integration with the Jerman filter. In another approach, Dash et al. [6] combined a homomorphic filter with CLAHE to effectively segment the retinal vascular system while maintaining a low computational cost.

Geethalakshmi et al. [25] investigated an alternative unsupervised method for retinal vessel segmentation, which combines CLAHE with median filtering to enhance the vascular structures. The core segmentation step was performed using maximum principal curvature analysis in conjunction with various morphological operations. Similarly, Jadoon et al. [26] and Nayab et al. [27] proposed unsupervised segmentation techniques that also begin with CLAHE-based contrast enhancement. Jadoon et al. [26] subsequently applied the Top-Hat morphological operation for noise reduction, followed by a sequence of High-Boost filtering, Frangi filtering, and ISODATA thresholding to generate the final binary vessel map. On the other hand, Nayab et al. [27] utilized Gabor wavelets in combination with a suitable filter and integrated a Human Visual System (HVS)-based approach to achieve robust vessel segmentation results.

Among supervised approaches, Zhang et al. [9] introduced a retinal vessel binarization model that leverages a combination of filtering techniques and wavelet transforms. Their method applies specialized transformations to enhance feature extraction by maximizing orientation responses across multiple scales, enabling effective detection of vessels with varying diameters. The final segmentation is performed using a Random Forest classifier. Similarly, Soares et al. [16] constructed feature vectors based on pixel intensities and the scaled responses of two-dimensional Gabor wavelets applied to local pixel neighborhoods. These feature vectors were then classified into vessel and non-vessel categories using a Bayesian classifier with Gaussian Mixture Models (GMM).

Aslan et al. [17] extracted retinal vessels directly from original fundus images by feeding key features into an Extreme Learning Machine (ELM). During the feature extraction stage, they applied adaptive thresholding, Gabor filtering, and Top-Hat transformations to enhance the vascular structures. In a different approach, Boudegga et al. [28] proposed a U-shaped deep learning architecture composed of simple convolutional blocks. Their model was designed to maintain

Journal of Information Systems Engineering and Management
2025, 10(4)
e-ISSN: 2468-4376
https://www.jisem-journal.com/

Research Article

high segmentation accuracy while reducing computational complexity, following a series of preprocessing operations. Comprehensive reviews of supervised retinal vessel segmentation techniques, particularly those based on neural networks and their variants, are available in Refs. [4], [29], [30] and [31].

Supervised methods particularly those based on deep learning—typically yield higher segmentation accuracy than their unsupervised counterparts. However, their implementation can be complex due to the requirements of large annotated datasets and high computational resources. To capitalize on the strengths of both paradigms, several researchers have proposed hybrid approaches that integrate supervised and unsupervised techniques to achieve more efficient and robust segmentation [18], [32]. Hashemzadeh et al. [32] introduced a hybrid segmentation framework that begins with an unsupervised phase aimed at detecting prominent and thick blood vessels. This is followed by a AND supervised phase that focuses on identifying thinner vessels. The method relies on a diverse set of image features including the Top-Hat transform, Shade Correction, Bit Plane Slicing, and Fuzzy C-Means clustering. The final output is refined through post-processing, which involves slightly reducing the radius of the field of view (FOV) mask. Fang et al. [18] also proposed a hybrid model, beginning with a supervised segmentation step using a Generalized Linear Model (GLM) combined with Gabor wavelet transforms. This was followed by an unsupervised phase involving contrast enhancement via CLAHE to manage illumination variations and enhance local details.

Drawing on numerous prior studies, this research introduces a hybrid segmentation approach that integrates the Frangi filter, a 2D convolution filter, and a FIR (UOI) filter, followed by Otsu's thresholding and morphological processing. By combining these methods, the system achieves a more balanced sensitivity and specificity, resulting in an enhanced AUC. Performance evaluation is conducted using sensitivity, specificity, and AUC metrics.

2. PROPOSED METHOD

In this study, we focused on the green channel of RGB fundus images, since blood vessels appear most distinct against the background in this channel, unlike the blue channel (which has limited dynamic range) and the red channel (which lacks sufficient contrast) Figure 1. Mendonça and Campilho [33] confirmed the superiority of the green channel by comparing it not only with other RGB channels but also with the NTSC luminance channel and the 'a' component of the Lab color space—and found that the green channel consistently provided the best overall contrast. As is standard in the field, we restrict segmentation to pixels within the image field of view (FOV); pixels outside this area are treated as background with no clinical relevance. Figure 2 presents a flowchart of the proposed methodology. The following sections provide a detailed breakdown of each processing step

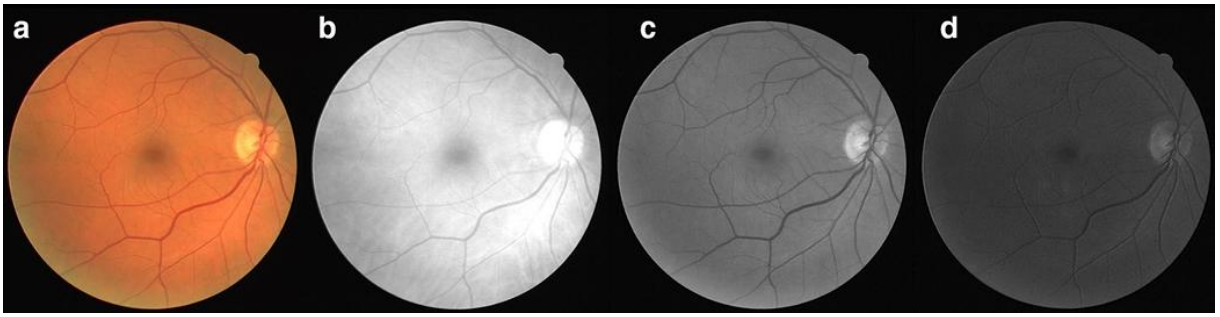

Figure 1: *Color fundus image and it's different RGB channels. a RGB image, b red channel, c green channel and d blue channel.*

Journal of Information Systems Engineering and Management
2025, 10(4)
e-ISSN: 2468-4376
https://www.jisem-journal.com/

Research Article

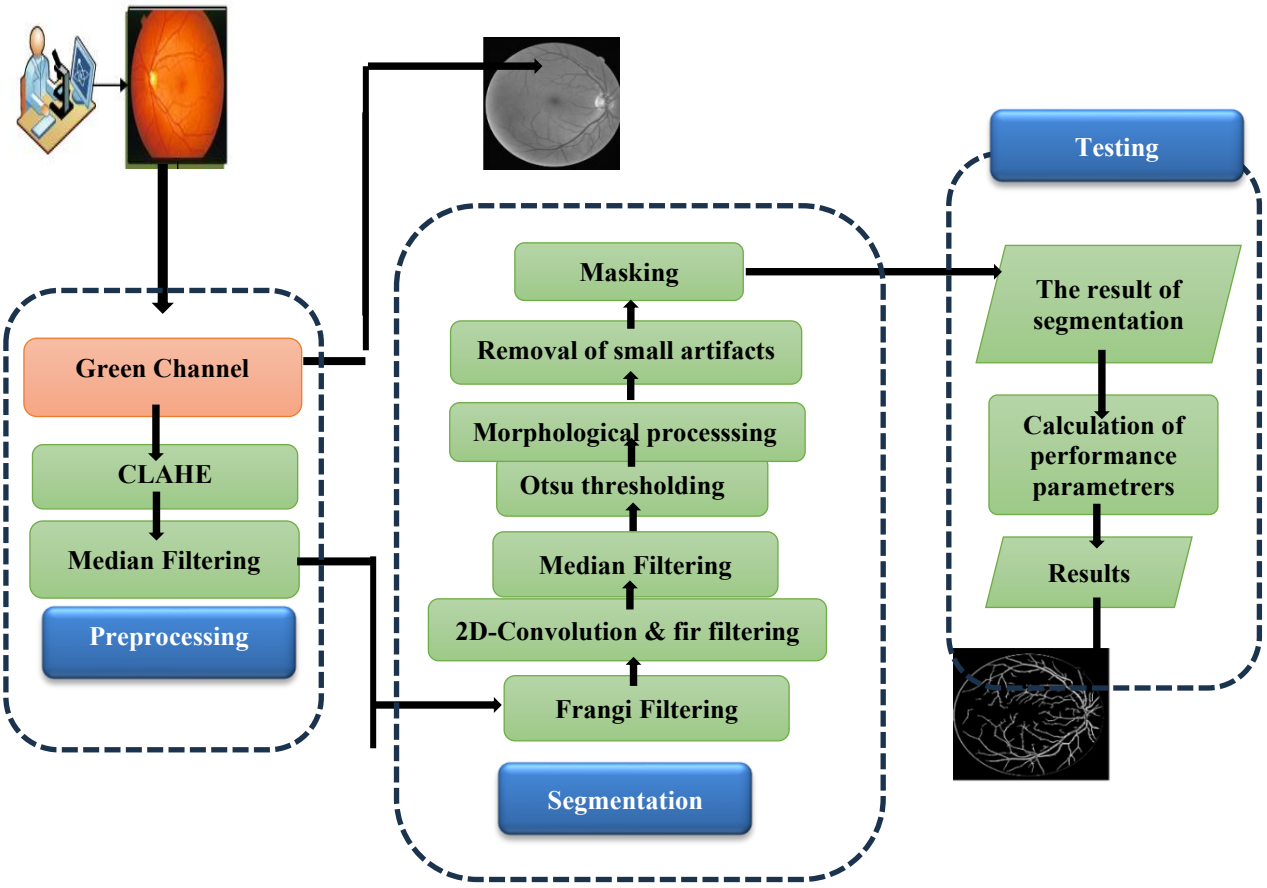

Figure 2: *Flowchart of the proposed model.*

2.1. Dataset

The DRIVE [34] and STARE [35]datasets—publicly available digital retinal image collections—are among the most widely used resources for developing and evaluating retinal vessel segmentation methods. Each dataset includes expert-generated manual segmentations of vessels, which serve as the ground truth reference.

The DRIVE dataset consists of 40 color fundus images, evenly split into training and testing subsets. Each image is accompanied by a field-of-view (FOV) mask and expert manual segmentation of the vessel tree—one expert for the training set and two experts for the testing set. The images were captured using a Canon CR5 non-mydriatic camera with a 45° FOV, 8-bit depth, and a resolution of 768×584 pixels. Figure 3 shows an example test image alongside its manual vessel segmentation.

The STARE dataset contains 20 color fundus images, half of which display various pathologies. Each image includes vessel-tree segmentations performed manually by two experts. These images were taken using a Canon TopCon TRV-50 fundus camera with a 35° FOV, 8-bit depth, and a resolution of 700×605 pixels. Figure 4 presents a representative image and its manual vessel segmentation.

Journal of Information Systems Engineering and Management
2025, 10(4)
e-ISSN: 2468-4376
https://www.jisem-journal.com/

Research Article

a b c

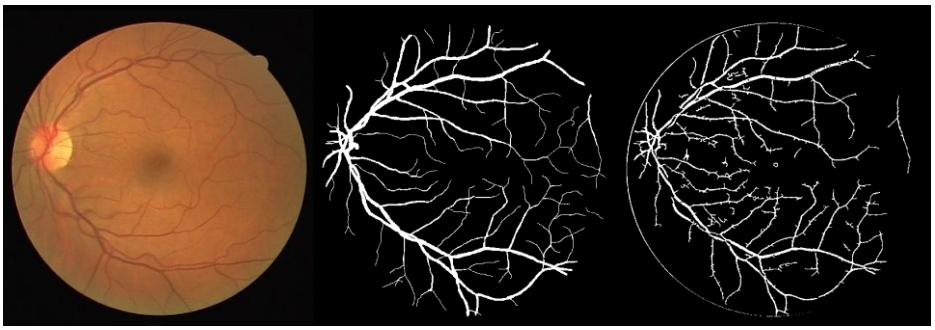

Figure 3: (*a)An image from the DRIVE test set with its respective manual vessel segmentation the (b) first observer and (c) second observer.*

a b c

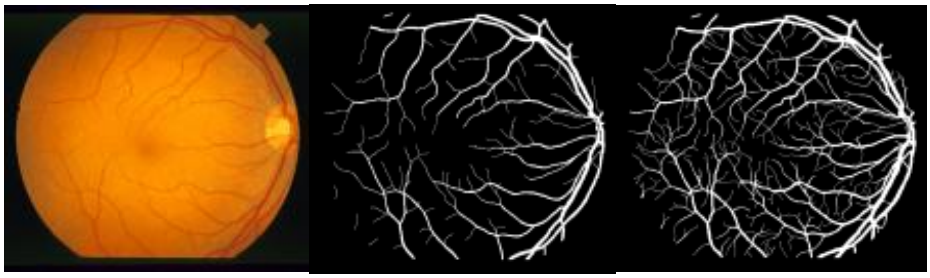

Figure 4: (*a) An image from the STARE test set with its respective manual vessel segmentation the (b) first observer and (c) second observer.*

2.2. Preprocessing:

Preprocessing retinal images typically begins with decomposing the image into red, green, and blue (RGB) channels—since the green channel often provides the highest contrast and clarity, it is used for further enhancement—followed by Contrast-Limited Adaptive Histogram Equalization (CLAHE) [36] [37], originally proposed by Zuiderveld, which divides the image into tiles, applies histogram equalization within each, and clips histogram peaks (commonly to limit amplification to a factor of ~3–4) to enhance local contrast and edge definition while suppressing noise amplification, in our experiments, we found that a 32×32 tile grid with a clip limit of 5.5 delivered optimal contrast improvement without introducing artifacts, and the final step applies a median filter to further reduce residual noise [37].

2.3. Frangi Filter:

The segmentation process encompasses various techniques, one of which is the Frangi filter. This filter is instrumental in detecting and enhancing blood vessels in retinal images. Given the varying diameters of retinal blood vessels, the Frangi filter analyzes each pixel to determine the scale at which the maximum response occurs, effectively highlighting vessel structures. This detection mechanism relies on the computation of the Hessian matrix, which evaluates second-order derivatives to identify tubular formations within the image [38].

The Hessian matrix kernel in the Frangi filter is designed to analyze scalar functions of multiple variables, identifying points where the function attains local maxima or minima under specific conditions. For a function f(x,y,z), the Hessian matrix is a 3×3 matrix comprising second-order partial derivatives, as illustrated in Equation (1). This matrix is particularly relevant for functions defined in three-dimensional space [38].

$$Hf(x,y,z) = \begin{bmatrix} \frac{\partial^2 f}{\partial x^2} & \frac{\partial^2 f}{\partial x \partial y} & \frac{\partial^2 f}{\partial x \partial z} \\ \frac{\partial^2 f}{\partial y \partial x} & \frac{\partial^2 f}{\partial y^2} & \frac{\partial^2 f}{\partial y \partial z} \\ \frac{\partial^2 f}{\partial z \partial x} & \frac{\partial^2 f}{\partial z \partial y} & \frac{\partial^2 f}{\partial z^2} \end{bmatrix} \quad (1)$$

Journal of Information Systems Engineering and Management
2025, 10(4)
e-ISSN: 2468-4376
https://www.jisem-journal.com/

Research Article

In the case of retinal images, it is enough to use 2 dimensions, namely f(x,y), so that the Hessian matrix is as shown in equation (2) [39].

$$Hf(x,y) = \begin{bmatrix} \frac{\partial^2 f}{\partial x^2} & \frac{\partial^2 f}{\partial x \partial y} \\ \frac{\partial^2 f}{\partial y \partial x} & \frac{\partial^2 f}{\partial y^2} \end{bmatrix} \quad (2)$$

the function f(x,y)is modeled as a two-dimensional Gaussian distribution, as presented in Equation (3). The Hessian matrix is constructed by computing the second-order partial derivatives of this Gaussian function.

$$f(x,y) = \frac{1}{2\pi\partial^2} e^{-[(x-x_0)^2+(y-y_0)^2]/(2\sigma^2)} \quad (3)$$

In this study, the eigenvalue decomposition of the Hessian matrix is employed to extract eigenvalues λ1 and λ2, which are instrumental in characterizing the local curvature of image structures. The scale parameter σ is pivotal in determining the appropriate scale for blood vessel detection. The Frangi filter's response is optimized when σ aligns with the actual size of the blood vessels; an incorrect σ value can diminish the filter's efficacy in vessel detection.

The Frangi vesselness function for two-dimensional images is defined in Equation (4):

$$V_f(s) = \begin{cases} 0 & if\ \lambda > 0 \\ \exp\left(-\frac{R_B}{\beta^2}\right)\left(1 - exp\left(-\frac{s^2}{2c^2}\right)\right) & otherwise \end{cases} \quad (4)$$

Here, $R_B = \frac{|\lambda_1|}{|\lambda_2|}$ quantifies the blob-like structure, and $s = \sqrt{\lambda_1^2 + \lambda_2^2}$ represents the second-order structureness. The parameters $\boldsymbol{\beta}$and $\boldsymbol{c}$ control the sensitivity of the filter to these measures. This formulation enhances the detection of tubular structures, such as blood vessels, by suppressing responses from blob-like or plate-like structures.

2.4. Convolution Filtering:

Convolution filtering is a two-dimensional operation fundamentally shaped by its kernel. Formally, the process can be expressed as in Equation (5):

$$G(x,y) = \sum_{s=-a}^{a} \sum_{t=-b}^{b} w(s,t) f(x-s, y-t) \quad (5)$$

Here, $G(x,y)$ is the filtered output, $f(x,y)$ is the original image, and $w(s,t)$ is the convolution kernel. The indices s and t each range from −a to +a and −b to +b, defining the neighborhood over which the kernel is applied. To enhance the clarity of blood vessels, this approach is combined with a two-dimensional Finite Impulse Response (FIR) filter—specifically, a circular averaging (pillbox) filter. This smooths the image uniformly within the defined radius, improving vessel quality.

2.5. Otsu's Thresholding:

The optimal threshold is the one that yields the lowest possible segmentation error. One widely used method for achieving optimal thresholding is Otsu's method [40]. Compared to other thresholding techniques, Otsu's method offers several advantages: it is computationally efficient, delivers strong performance when combined with other image processing methods, and maintains stable results across various applications [41]. Otsu's algorithm automatically determines the optimal threshold by assuming that the image histogram is bimodal, meaning it represents two distinct pixel classes—typically foreground and background. The method works by minimizing the intra-class variance between these two-pixel classes [42].

The intra-class variance equation is given by:

$$\sigma^2(t) = q_1(t)\sigma_1^2(t) + q_2(t)\sigma_2^2(t) \quad (6)$$

where $q_1(t)$ and $q_2(t)$ are the probabilities of the two classes (background and foreground), and $\sigma_1^2(t)$, $\sigma_2^2(t)$ are their respective variances. These class probabilities and variances are calculated using the following equations:

Journal of Information Systems Engineering and Management
2025, 10(4)
e-ISSN: 2468-4376
https://www.jisem-journal.com/

Research Article

$$q_1(t) = \sum_{i=0}^{t} P(i) \quad (7)$$

$$q_2(t) = \sum_{i=t+1}^{k} P(i) \quad (8)$$

$$\sigma_1^2(t) = \sum_{i=0}^{t} [i - \mu_1(t)]^2 . \frac{P(i)}{q_1(t)} \quad (9)$$

Where $\mu_1(t)$ and $\mu_2(t)$are the class means, given by:

$$\mu_1(t) = \frac{\sum_{i=0}^{t} iP(i)}{q_1(t)} \quad (10)$$

$$\mu_2(t) = \frac{\sum_{i=t+1}^{k} iP(i)}{q_2(t)} \quad (11)$$

Here, $P(i)$ denotes the probability of pixel intensity i, and k is the maximum intensity value (typically 255 for 8-bit images). As illustrated in Figure 2, the Otsu thresholding method is applied after the Frangi filtering stage, followed by morphological image processing. In this study, the threshold value obtained via Otsu's method is normalized on a scale from 0 to 1.

2.6. Morphological Processing:

Morphological processing refers to operations that modify the structural shape of objects within an image. These operations involve two two-dimensional matrices: the first is the input image to be processed, and the second is the structuring element or kernel. In this study, three morphological operations are employed: closing, diagonal fill, and bridging unconnected pixels. The closing operation is defined by the mathematical model in Equation (12). This operation consists of a dilation followed by an erosion, and is typically used to fill small holes and connect adjacent structures [43].

$$A.B = (A \oplus B) \ominus B \quad (12)$$

The diagonal fill operation is applied to remove background connectivity via 8-connected neighbors, which helps isolate meaningful structures. The bridging operation aims to connect previously unlinked pixels by setting a pixel with value 0 to 1 if it has two non-zero neighbors that are not directly connected—effectively filling small gaps in vessel structures. These binary morphological operations are used to refine the output from the Otsu thresholding step, specifically by eliminating non-vessel pixels and enhancing the continuity and clarity of blood vessels.

2.7. Evaluation criteria :

The effectiveness of any vascular segmentation method depends on its ability to accurately distinguish vessel pixels from background pixels. To evaluate performance, the segmentation results are compared against manually annotated binary ground-truth masks, which serve as reference standards. This pixel-level comparison yields four fundamental outcomes:

- **True Positive (TP):** Vessel pixels correctly identified as vessels.
- **False Negative (FN):** Vessel pixels incorrectly classified as background.
- **True Negative (TN):** Background pixels correctly identified as background.
- **False Positive (FP):** Background pixels incorrectly classified as vessels.

These four categories are essential for evaluating the performance of any vascular segmentation method. From these values, various performance metrics are derived to quantitatively compare the proposed technique with state-of-the-art methods:

Sensitivity (Sn) or True Positive Rate (TPR): Indicates the method's effectiveness in detecting vessel pixels.

$$Sensitivity = \frac{TP}{TP+FN} \quad (13)$$

Specificity (Sp): Measures the accuracy of background pixel classification.

$$Specificity = \frac{TN}{TN+FP} \quad (14)$$

Journal of Information Systems Engineering and Management
2025, 10(4)
e-ISSN: 2468-4376
https://www.jisem-journal.com/

Research Article

Accuracy: Represents the proportion of correctly classified pixels (both vessels and background) relative to the total number of pixels in the Field of View (FOV).

$$Accuracy = \frac{TP+TN}{TP+FN+TN+FP} \quad (15)$$

Another widely used performance metric is the Area Under the Curve (AUC), derived from the Receiver Operating Characteristic (ROC) curve by evaluating performance across varying threshold values. However, AUC is not applicable in our case, as we treat the segmentation of large and small vessels as separate binary classification problems. These results are then linearly combined to generate the final segmentation output.

2.8. Environment Setup

We used Google's free cloud services to implement the proposed model—outstanding tools for image processing with Python. The services we employed include the "Google Colab" cloud which is a platform hosting open source "Jupyter notebooks" with free GPU support and "Google Drive" cloud storage solution used to upload and store our image datasets, which can be easily mounted and accessed directly from within Colab.

3. Results And Discussion

Research using the method illustrated in Figure 2 yielded several outputs. Initially, segmentation results are displayed in Figure.5 , which depicts the test outcomes on the DRIVE dataset. Figure 5 shows the results of main processing phases of proposed approach for an image sample using the DRIVE database. Figure 6 shows the results of main processing phases of proposed approach for an image sample using the STARE database, respectively.

The subsequent output was the performance evaluation of our proposed system, conducted using two benchmark datasets: DRIVE and STARE. We assessed performance based on three key metrics—sensitivity, specificity, and accuracy—as defined in Equations (13-15). The evaluation used a sample set of 20 retinal images. For each image, segmentation results produced by our model were compared against manually annotated segmentations provided by expert graders in both datasets. The numerical results for all 20 cases are compiled in Table I.

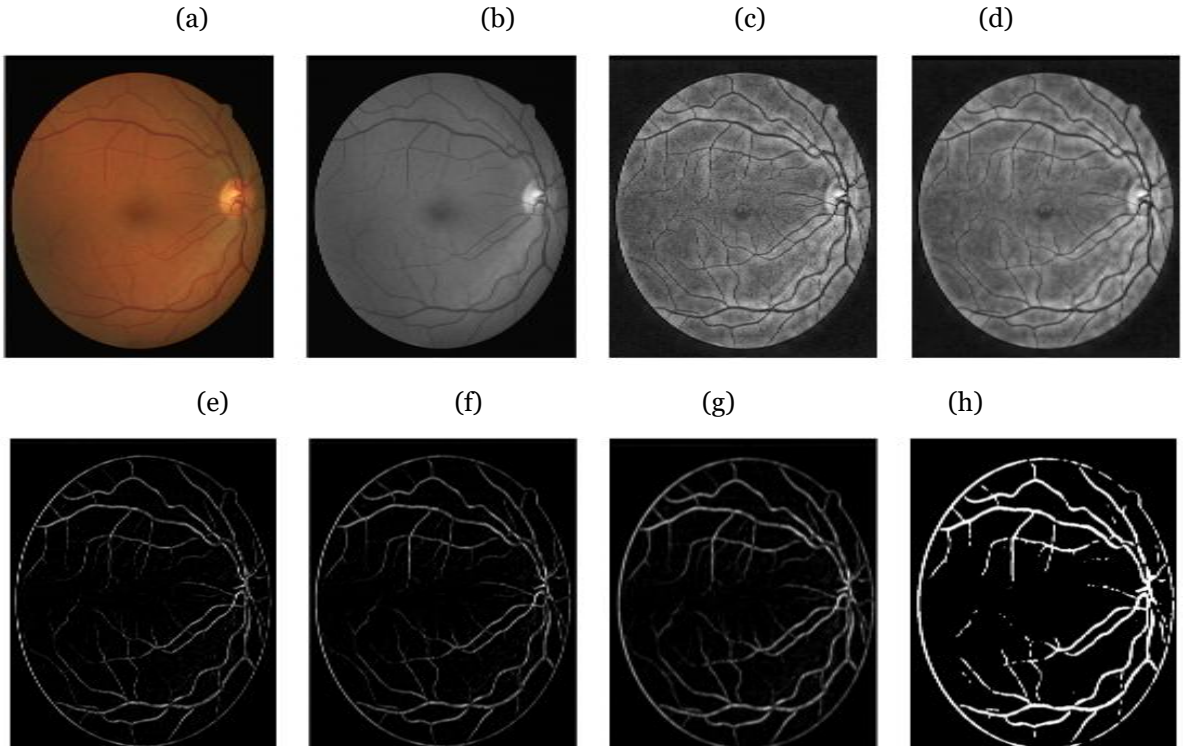

Journal of Information Systems Engineering and Management
2025, 10(4)
e-ISSN: 2468-4376
https://www.jisem-journal.com/

Research Article

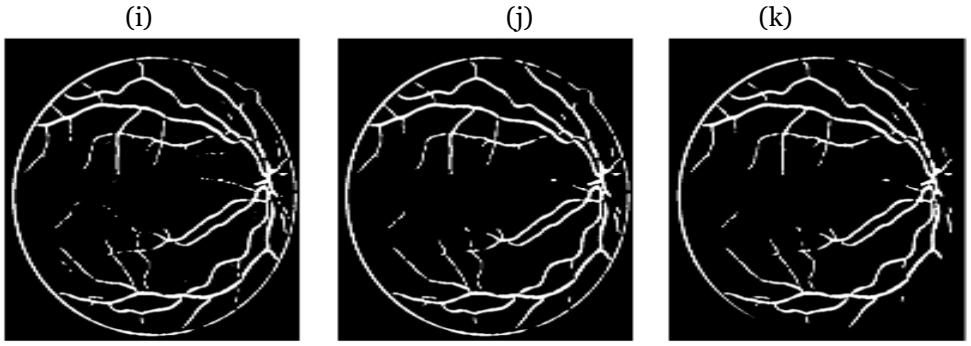

Figure. 5: *Visual inspection of the processing steps of the proposed system using the DRIVE database: (a) the original image, (b) the green channel, (c) the image after CLAHE enhanced, (d) the image after Median filter, (e) the image after Frangi filter, (f) the image after 2D CONV, (g) the image after Fir filtering, (h) the image after Otsu, (i) Post-processing operation, (j) cleaned image, (k) the final image.*

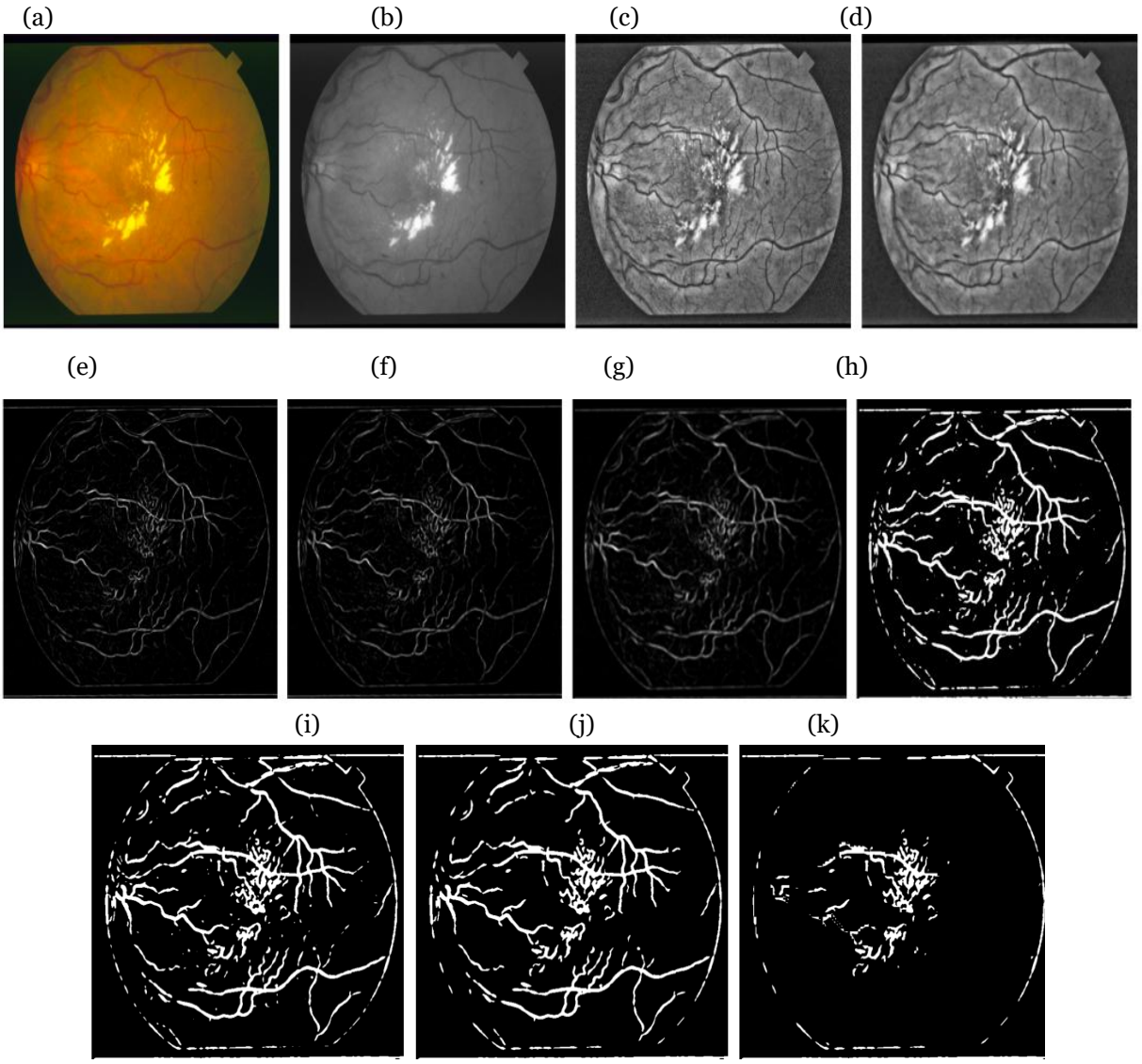

Figure. 6 *Visual inspection of the processing steps of the proposed system using the SARE database: (a) the original image, (b) the green channel, (c) the image after CLAHE enhanced, (d) the image after Median filter, (e) the image after Frangi filter, (f) the image after 2D CONV, (g) the image after Fir filtering, (h) the image after Otsu, (i) Post-processing operation, (j) cleaned image, (k) the final image*

Journal of Information Systems Engineering and Management
2025, 10(4)
e-ISSN: 2468-4376
https://www.jisem-journal.com/

Research Article

3.1.Discussion

Tests of the proposed segmentation model on both the DRIVE and STARE datasets revealed consistent performance differences. On DRIVE, specificity was notably higher than sensitivity, meaning the system more reliably identifies background pixels (true negatives) than blood-vessel pixels (true positives). Overall accuracy reached **94 %**, confirming the model's strong general pixel classification capability. For STARE, performance dipped somewhat. This is understandable, as STARE contains more delicate and intricate vessel structures that are harder to distinguish from the background compared to DRIVE. Consequently, while sensitivity and specificity are both affected, the model still maintains a respectable overall accuracy of approximately **90 %**.

We note sensitivity is limited by the challenge of accurately selecting the Frangi filter parameters c and β (see Equation 4). When these parameters are paired incorrectly, they can counteract each other, resulting in suboptimal performance. Table I results were obtained through manual tuning across various (c,β) combinations. The optimal values identified were: c= (1, 15); β=5. However, manual parameter selection is inefficient and prone to error. To automate and improve this tuning process, one could apply computational intelligence optimization—such as genetic algorithms, particle swarm optimization, or ant colony optimization. This would allow the system to systematically and adaptively find the optimal (c,β) pair based on performance feedback, eliminating reliance on manual experimentation and ensuring more consistent results.

NUM	**DRIVE**			**STARE**		
	ACC	**SP**	**SN**	**ACC**	**SP**	**SN**
1	0.9555	0.9810	0.6390	0.9710	0.7602	0.5494
2	0.9449	0.9790	0.6008	0.9755	0.7248	0.4741
3	0.9177	0.9382	0.6269	0.9738	0.7683	0.5628
4	0.9320	0.9826	0.5457	0.8704	0.9003	0.9301
5	0.9345	0.9854	0.4554	0.9531	0.8579	0.7628
6	0.9426	0.9777	0.5575	0.8779	0.8799	0.8819
7	0.9452	0.9761	0.6256	0.8999	0.9039	0.9079
8	0.9384	0.9716	0.6320	0.9030	0.8811	0.8593
9	0.9485	0.9808	0.5966	0.9068	0.9110	0.9152
10	0.9463	0.9848	0.4948	0.8583	0.9074	0.9566
11	0.9524	0.9744	0.6106	0.9087	0.8721	0.8355
12	0.9558	0.9865	0.6116	0.8891	0.9114	0.9338
13	0.9491	0.9764	0.6393	0.8746	0.8970	0.9194
14	0.9020	0.9375	0.5741	0.8502	0.8858	0.9213
15	0.9468	0.9697	0.7053	0.8890	0.8548	0.8206
16	0.9382	0.9790	0.6035	0.8691	0.8949	0.9206
17	0.9343	0.9565	0.7026	0.9886	0.7079	0.4272
18	0.9505	0.9806	0.6323	0.8614	0.8699	0.8784
19	0.9449	0.9752	0.6230	0.9194	0.8554	0.7915
20	0.9564	0.9799	0.6699	0.8965	0.8702	0.8439
MEAN	**0.9418**	**0.9736**	**0.6073**	**0.9086**	**0.8557**	**0.8046**

Journal of Information Systems Engineering and Management
2025, 10(4)
e-ISSN: 2468-4376
https://www.jisem-journal.com/

Research Article

TABLE I: *Testing Results Using Dataset*

AUTHOR	ACC	SP	SN
DASH ET AL. [6]	0.7203	NAN	NAN
SHIN [44]	0.9271	0.9255	0.9382
ROYETAL [45]	0.9295	0.4392	0.9622
WIHARTO [46]	0.8904	0. 8689	0. 9118
APPROACH 1	**0.9418**	**0.9736**	**0.6073**

Table 2: Comparison of experimental results of different algorithms on DRIVE.

AUTHOR	ACC	SP	SN
DASH ET AL. [6]	0.6454	NAN	NAN
NUGROHO [47]	0.8876	0.9038	0.7550
ROYETAL [45]	0.9488	0.4317	0.9718
APPROACH 2	**0.9086**	**0.8557**	**0.8046**

Table 3: Comparison of experimental results of different algorithms on STARE

For comparison with the previous vessel detection methods, experiments were conducted on DRIVE and STARE datasets, and their performance evaluation metrics were gauged. An objective comparison follows in the forms of tables 2 and 3 where the performance parameters are compared with other top vessel segmentation strategies. the performance of the proposed hybrid segmentation model, evaluated using the ACC metric, demonstrates capabilities superior to several previous studies, as shown in Table II. It is also comparable to the results reported by Wiharto [45]. However, Wiharto's study relies on a combination of multiple methods—Frangi filter, median filter, and Otsu—which entails high computational complexity and longer processing times to achieve such performance.

The comparison continues with the work of Dash et al. [6], where the authors combined a homomorphic filter with CLAHE to effectively segment the retinal vascular system while maintaining low computational cost. On the DRIVE dataset, they achieved an ACC of 0.7203, which remains lower than the performance of our model. Similarly, in the study by Roy et al. [24], although their method achieves high sensitivity (up to 97.6%), their specificity remains lower than that of our model, and their overall accuracy is also inferior.

For the STARE database, the proposed method achieves acceptable scores, with sensitivity (Sn) of 0.8046, specificity (Sp) of 0.8557, and precision of 0.9086—values comparable to those of the top competitors in their respective categories. It is also worth noting that some techniques achieve high scores in certain metrics but often at the expense of other performance indicators.

CONCLUSION AND FUTURE WORK

Automated vessel segmentation is a foundational step in retinal image analysis. Once the vasculature is extracted, it enables precise measurements such as vessel diameter, tortuosity, and the distinction between arteries and veins to compute the arteriovenous ratio. Additionally, these segmented vessels serve as essential features in systems designed to diagnose retinal diseases and detect systemic conditions like diabetes, stroke, and hypertension.

In this paper, we propose a fully unsupervised approach for blood vessel segmentation in retinal images, validated on the DRIVE and STARE databases. Our preprocessing consists of three sequential steps: Green-channel extraction, which provides a uniform basis for further processing, CLAHE (Contrast Limited Adaptive Histogram Equalization) to enhance image contrast, Median filtering to reduce noise. Following preprocessing, segmentation is performed through a hybrid pipeline that includes: A Frangi filter to enhance vessel-like tubular structures, Otsu's thresholding for automatic binarization of the enhanced image, and Morphological operations to close gaps, remove small artifacts,

and ensure continuity of the vessel network. This combined Frangi–Otsu–morphological pipeline effectively segments retinal blood vessels in both the DRIVE and STARE datasets. Experimental results demonstrate accuracies of 0.9418 on DRIVE and 0.9086 on STARE, with corresponding specificity values of 0.9736 and 0.8557. Comparative analysis indicates that our model offers statistically competitive performance relative to established methods in the literature. Importantly, our algorithm relies on straightforward processing techniques that are easy to implement, making it highly suitable for automated workflows. This facilitates the optimization of diagnostic tools for various retinal disorders.

The proposed model, evaluated using the ACC metric, presents a promising alternative for retinal blood vessel segmentation. Its performance can be further improved by fine-tuning the c and β parameters of the Frangi filter. Future work could leverage optimization algorithms—such as Particle Swarm Optimization—to automatically identify these optimal parameter values.

REFERENCES

[1] R. Imtiaz, T. Khan, S. Naqvi, , M. Arsalan et S. Nawaz, «Screening of Glaucoma disease from retinal vessel images using semantic segmentation,,» *Comput. Electr. Eng,* vol. 91, p. 107036, 2021.

[2] J. Tan, . U. Acharya, S. Bhandary et . K. Chua, «, Segmentation of optic disc, fovea and retinal vasculature using a single convolutional neural network,» *Journal of Computational Science ,* vol. 20, p. 70–79, 2017.

[3] K. Sil et . S. Maity, «Extraction of retinal blood vessel using curvelet transform and fuzzy c-means,,» chez *22nd International Conference on Pattern Recognition, IEEE,*, 2014.

[4] N. Salamat, . M. Missen et . A. Rashid, «Diabetic retinopathy techniques in retinal images a review,,» *Artif. Intell. Med. ,* vol. 97, pp. 168–188,, 2019.

[5] B. Zhang, L. Zhang et F. Karray, «Retinal vessel extraction by matched filter with first-order derivative of Gaussian,» *Comput. Biol. Med,* vol. 4, p. 40 , 2010.

[6] s. Dash, M. Senapati, P. Sahu et P. Chowdary, «Illumination normalized based technique for retinal blood vessel segmentation,,» *Int. J. Imag. Syst. Technol,* vol. 31, n° %11, p. 351–363, 2021.

[7] N. Ibrahim, A. El Farag et R. Kadry, «Gaussian blur through parallel computing,» chez *Proceedings of the International Conference on Image Processing and VisionEngineering* , 511 (1) (2021) 978–989, .

[8] C. Ravichandran et . J. Raja, «A fast enhancement/thresholding based blood vessel segmentation for retinal image using contrast limited adaptive histogram equalization.,» *J. Med. Imaging Health Inform.,* vol. 4 , n° %14 , p. 567–575, 2014.

[9] J. Zhang, Y. Chen, E. Bekkers, M. Wang et B. Dashtb, «Retinal vessel delineation using a brain-inspired wavelet transform and random,» *Pattern Recogn.,* vol. 69, pp. 107-123, 2017.

[10] K. Asem, A. Ramli, S. Hashim et Z. Noh, «Image denoising algorithm using second generation wavelet transformation and principle component analysis,» chez *Res. J. Appl. Sci. Eng. Technol.*, 2014.

[11] Z. Zhen, S. Ma, H. Liu, et Y. Gong, «An edge detection approach based on directional wavelet transform,,» *Comput. Math. Appl.,* vol. 57, n° %18, p. 1265–1271, 2009.

[12] P. Bankhead, C. Scholfield et J. J.G. McGeown, «Fast retinal vessel detection and measurement using wavelets and edge location refinement,,» *PLoS One,* vol. 7, n° %13, 2012.

[13] K. Sil. et S. Maity, «Extraction of retinal blood vessel using curvelet transform and fuzzy c-means,,» chez *22nd International Conference on Pattern*, 2014.

[14] A. Rahulkar, D. Jadhav et R. Holqmbe, «Fast discrete curvelet transform based anisotropic feature extraction for iris recognition,» *ICTACT Journal on Image and Video Processing ,* vol. 2, p. 69–75, 2010.

[15] A. Altan et S. Karasu, «Recognition of covid-19 disease from x-ray images by hybrid model consisting of 2D curvelet transform, chaotic salp swarm algorithm and deep learning technique,,» *Chaos, Solit. Fractals ,* vol. 140, n° %1 110071, 2020.

[16] C. Junior, H. Jelinek et M. Cree, «Retinal vessel segmentation using the 2D gabor wavelet and supervised classification,» *IEEE Trans. Med. Imag. ,* vol. 25, n° %19, p. 1214–1222, 2006.

[17] M. Aslan, M. Ceylan et A. Durdu, «Segmentation of retinal blood vessel using gabor filter and extreme learning

machines,» chez *International Conference on Artificial Intelligence and Data Processing (IDAP), IEEE* , 2018.

[18] L. Fang, L. Zhang et Y. Yao, «Retina blood vessels segmentation based on the combination of the supervised and unsupervised methods, Multidimens.,» *Syst. Signal Process.,* vol. 32, p. 1123–1139, 2021.

[19] l. Zhang, M. Fisher et W. Wang, «Retinal Vessel Segmentation Using Gabor,» chez *Medical Image Understanding and Analysis*, 2014.

[20] S. Dash , S. Verma, Kavita,, M. Khan et M. Wozniak, «A hybrid method to enhance thick and thin vessels for blood vessel segmentation,,» *Diagnostics,* vol. 11, n° %111, p. 2017, 2021.

[21] M. Tavakoli, A. Mehdizadeh, S. Pourreza et J. Dehm, «Unsupervised automated retinal vessel segmentation based on Radon line detector and morphological reconstruction,» *,IET Image Process.,* n° %17, p. 15, 2021.

[22] J. Dash et N. Bhoi, «An unsupervised approach for extraction of blood vessels from fundus images,,» *J. Digit. Imag.,* vol. 31 , p. 857–868, 2018.

[23] C. Ravichandran et J. Raja, «A fast enhancement/thresholding based blood vessel segmentation for retinal image using contrast limited adaptive histogram equalization,,» *J. Med. Imaging Health Inform. ,* vol. 4, n° %14, p. 567–575, 2014.

[24] M. Saleh, C. Eswaran et A. Mueen, «An automated blood vessel segmentation algorithm using histogram equalization and automatic threshold selection,,» *J. Digit. Imag,* vol. 24, n° %14, p. 564–572, 2010.

[25] K. Geethalakshmi et V. Meenakshi, «Mathematical morphology and optimum principal curvature based segmentation of blood vessels in human retinal fundus images,» *International Journal of Innovative Technology and Exploring Engineering,* vol. 8, n° %112, pp. 3034-3040, 2019.

[26] Z. Jadoon, S. Ahmad, M. Jadoon, A. Imtiaz, N. Muhammad et Z. Mahmood, «Retinal blood vessels segmentation using isodata and high boost filter,,» chez *3rd International Conference on Computing, Mathematics and Engineering Technologies (iCoMET) 29 1–6*, 2020.

[27] D. Dharmawan, D. Li, B. Ng et S. Rahardja, «A new hybrid algorithm for retinal vessels segmentation on fundus images,,» *IEEE Access,* vol. 7, pp. 41885–41896,, 2019.

[28] H. Boudegga, Y. Elloumi, M. Akil et M. Hedi Bedoui,, «Fast and efficient retinal blood vessel segmentation method based on deep learning network,,» *Comput. Med. Imag. Graph.,* vol. 90, n° %1101902, 2021.

[29] M. Krithika alias AnbuDevi et K. Suganthi, «Review of semantic segmentation of medical images using modified architectures of UNET,» *Diagnostics,* vol. 12, n° %112, p. 3064, 2022.

[30] c. Chen, J. Chuah, R. Ali et Y. Wang, «Retinal vessel segmentation using deep learning: a review,,» *IEEE Access,* vol. 9, p. 111985–112004, 2021.

[31] A. Ilesanmi, T. Ilesanmi et . A. Gbotoso, «A systematic review of retinal fundus image segmentation and classification methods using convolutional neural networks,» *Healthcare Analytics,* vol. 100261, 2023.

[32] M. Hashemzadeh et B. Azar, «Retinal blood vessel extraction employing effective image features and combination of supervised and unsupervised machine learning methods,» *Artif. Intell. Med. ,* vol. 95, pp. 1–15,, 2019.

[33] A. Mendonca et A. Campilho, «Segmentation of retinal blood vessels by combining the detection of centerlines and morphological reconstruction,» *IEEE Transactions on Medical Imaging,* vol. 25(9), p. 1200–1213., 2006.

[34] J. Staal, M. Abràmoff , M. Niemeijer , M. Viergev et B. Van Ginneken, «Ridge-based vessel segmentation in color images of the retina,» *IEEE Transactions on Medical Imaging,* vol. 23(4), p. 501–509., 2004.

[35] A. Hoover, V. Kouznetsova et M. Goldbaum, «Locating,» 2000.

[36] J. Ma , X. Fan , S. Yang , X. Zhang et X. Zhu, «Contrast Limited Adaptive Histogram Equalization-Based Fusion in YIQ and HSI Color Spaces for Underwater Image Enhancement,» *Int. J. Pattern Recognit. Artif. Intell., ,* Vols. %1 sur %2vol. 32, no. 7, 2018.

[37] K. Noronha , K. Navya et K. Nayak , «Support system for the Automated detection of hypertensive retinopathy using fundus images,» *In International Conference on Electronic Design and Signal Processing (ICEDSP),,* pp. Manipal, India, pp. 7–11, 2012.

[38] F. Sabaz et U. Atila, «Roi Detection And Vessel Segmentation In Retinal Image.,» *ISPRS - Int. Arch. Photogramm. Remote Sens. Spat Inf. Sci,* Vols. %1 sur %2vol. XLII-4/W6, pp. pp. 85–89,, 2017.

Research Article

[39] P. Truc, M. A. U. Khan, Y. Lee et S. Lee, «Vessel enhancement filter using directional filter bank,» *comput. vis. image Underst.,* Vols. %1 sur %2 vol. 113, no. 1, p. pp. 101–112, 2009.

[40] N. Otsu, «A Threshold Selection Method from Gray-Level Histograms,» *IEEE Trans. Syst. Man Cybern,* Vols. %1 sur %2vol. 9, no. 1, p. pp. 62–66, 1979.

[41] W. Kang, Q. Yang et R. Liang, «The Comparative Research on Image Segmentation Algorithms,» chez *First International workshop on Education Technology and Computer Science, Wuhan,* , Hubei, China. pp. 703–707., 2009.

[42] M. Ansari et S. Mahraj , «A Robust Methodfor Identification of Paper Currency Using Otsu's Thresholding,» chez *International Conference on Smart Computing and Electronic Enterprise (ICSCEE),* , Shah Alam, Malaysia, pp. 1–5. , 2018.

[43] F. Y. Shih, «Image Processing and Mathematical Morphology Fundamentals and Applications. Boca Raton.,» *CRC Press,,* 2009.

[44] S. Shin, S. Lee, I. Yun et K. Lee, «Deep vessel segmentation by learning graphical connectivity,» *Med. Image Anal,* Vols. %1 sur %2vol. 58, no. 101556. , 2019.

[45] S. Roy, A. Mitra et S. Setua, «Blood vessel segmentation of retinal image using Clifford matched filter and Clifford convolution,» *Multimed. Tools Appl,* vol. 78, p. 34839–34865., 2019.

[46] Wiharto et Y. Palgunadi, «Blood Vessels Segmentation in Retinal Fundus Image using Hybrid Method of Frangi Filter, Otsu Thresholding and Morphology,» *International Journal of Advanced Computer Science and Applications, ,* Vols. %1 sur %2Vol. 10, No. 6, , 2019.

[47] H. Nugroho, R. Aras, T. Lestari et I. Ardiyanto, «Retinal Vessel Segmentation Based on Frangi Filter and Morphological Reconstruction,» chez *International Conference on Control, Electronics Renewable Energy and Communications (ICCEREC)*, 2017..